J Therm Anal Calorim (2012) 107:1293–1299
DOI 10.1007/s10973-011-1608-4

Phase transition at thermal dehydration in stilbite

V. A. Drebushchak · S. N. Dementiev · Yu. V. Seryotkin

Received: 21 February 2011 / Accepted: 19 April 2011 / Published online: 7 May 2011

Abstract Thermal dehydration of stilbite was investigated by thermogravimetry and in situ X-ray powder diffraction. Sample mass changes continuously over the whole temperature range, with anomaly near 175 °C described in terms of the second-order phase transition with changes in symmetry from *F*-centered unit cell to *A*-centered one. This contradicts to the step-wise change in sample mass and the first-order phase transition with symmetry changing from *F*2/*m* to *Amma* reported in literature. The change in the order of the phase transition by means of the changes in experimental techniques is discussed.

Keywords Dehydration · Phase transition · Stilbite · Thermogravimetry · X-ray powder diffraction

Introduction

Natural zeolites are the framework aluminosilicates with rather large amount of water molecules inside cavities and channels, up to 20% by weight [1–3]. Thermal dehydration of zeolites is usually accompanied with the contraction of their unit cell (UC). The contraction and mass loss itself vary in the absolute value (large or small) and in the temperature function (smooth or step-wise) [4]. It is impossible to predict the contraction as a function of the water content or/and temperature even having the whole information about chemical composition and structure of the zeolite.

Thermal dehydration of zeolites was investigated for many decades with many experimental techniques (derivatography, TG, DSC, and TMA) [5–9]. The results of these investigations are the peak temperatures and mass loss, total or over particular temperature range. Large variations in the chemical composition of a zeolite species result in the wide range of the values of mass loss and peak temperatures and even in the number of the peaks.

Stilbite, $NaCa_4(Al_9Si_{27}O_{72})\cdot 30H_2O$, is monoclinic (*C*2/*m*) and closely connected with stellerite, $Ca_4(Al_8Si_{28}O_{72})\cdot 28H_2O$, orthorhombic (*Fmmm*) [10]. To make easy the comparison between these two species, the structure of stilbite is usually reported and discussed in pseudoorthorhombic doubled UC with non-standard space group *F*2/*m*. Thermal dehydration is nearly the same for stilbite and stellerite, with two close peaks one by one. The first one (~200 °C) is narrow and high and the second one (~250 °C) is broader and smaller. The first peak was reported to be the first-order phase transition with the step change of 3.24% in the UC volume and the change in symmetry from *C*2/*m* to *Amma* [11].

The objective of this work is to show that the phase transition in stilbite during thermal dehydration may be of the second order, without increasing symmetry.

Experimental

Materials

Stilbite (the Nidym river, basin of the Nizhnyaya Tunguska river, East Siberia, Russia) was presented with large (up to

V. A. Drebushchak (✉) · S. N. Dementiev · Yu. V. Seryotkin
Institute of Geology and Mineralogy SB RAS, Pr. Ac. Koptyuga 3, Novosibirsk, Russia 630090
e-mail: dva@igm.nsc.ru; dva@xray.nsu.ru

Yu. V. Seryotkin
e-mail: yuvs@igm.nsc.ru

V. A. Drebushchak · Yu. V. Seryotkin
Novosibirsk State University, Ul. Pirogova 2, Novosibirsk, Russia 630090

4 cm) white crystals. The composition of the sample was measured with "Camebax-micro" analyzer and found to correspond to $Ca_{3.98}Na_{1.10}[Al_{9.07}Si_{26.93}O_{72}]\cdot 29.0H_2O$, averaged after 11 analyses.

The structure of our stilbite was determined using X-ray single-crystal diffraction data. The crystals were checked for twinning under polarizing microscope. Final selection of the crystal was done on the basis of Laue X-ray diffraction data. A single crystal fragment of 0.07 × 0.12 × 0.18 mm was used for the data collection on an Enraf–Nonius CAD4 diffractometer with graphite-monochromatized MoKα radiation and ω scan ($\theta_{max} = 27°$). The data collection and structure determination were carried out in the non-standard space group *F2/m* (unit-cell parameters are $a = 13.5860(10)$, $b = 18.214(3)$, $c = 17.798(2)$ Å, $\beta = 90.67(1)°$, $Z = 2$). The intensities of 2158 non-equivalent reflections were measured; with 1624 observed ($I > 2\sigma(I)$). The structure was solved and refined with SHELX-97 program [12]. The positions of framework atoms and extraframework cations were refined with neutral atomic scattering factors in the anisotropic approximation (excluding low-populated Na-position). The T-position occupancy by Si and Al was estimated by the method described in [13]. The positions of water molecules were recognized using "pseudo-atomic" scattering factor for H_2O molecule [14]. Final $R_1 = 0.0376$ and $wR_2 = 0.0759$ for observed reflections and $R_1 = 0.0507$ and $wR_2 = 0.0797$ for all data. The structure of our stilbite is reported in the Tables 1 and 2 contain the coordinates, displacement parameters and occupancies for the atomic positions. T–O distances and T–O–T angles are listed in Table 3. Table 4 contains the interatomic distances less than 3 Å. The structural data are deposited as CIF at the ICSD (CSD-no. 422571).

Table 1 Atomic coordinates, equivalent isotropic displacement parameters $U_{eq} = 1/3\ \Sigma_i(\Sigma_j(U_{ij}\ a_i * a_j * a_i a_j))$ (Å^2) and the occupancies for atoms in stilbite

Atom	Occupancy	*x*	*y*	*z*	U_{eq}/Å^2
T11	$Si_{0.79}Al_{0.21}$	0.38404(7)	0.30912(5)	0.38017(5)	0.0148(2)
T12	$Si_{0.59}Al_{0.41}$	0.61240(7)	0.30526(5)	0.37268(5)	0.0146(2)
T2	$Si_{0.67}Al_{0.33}$	0.30163(7)	0.41117(5)	0.50598(5)	0.0143(2)
T3	$Si_{0.85}Al_{0.15}$	0.38854(7)	0.18338(5)	0.49952(5)	0.0136(2)
T4	$Si_{0.88}Al_{0.12}$	0.2500	0.25889(7)	0.2500	0.0179(3)
O11	1	0.30844(17)	0.31266(12)	0.30779(12)	0.0275(6)
O12	1	0.67437(18)	0.29411(12)	0.29384(13)	0.0294(6)
O21	1	0.37063(17)	0.23119(13)	0.42375(12)	0.0300(6)
O22	1	0.62608(18)	0.23262(13)	0.42688(12)	0.0335(7)
O31	1	0.36129(18)	0.37874(12)	0.43374(12)	0.0320(7)
O32	1	0.65120(18)	0.38140(12)	0.41481(12)	0.0294(6)
O4	1	0.49498(17)	0.31591(13)	0.34766(12)	0.0269(6)
O5	1	0.31542(17)	0.11326(11)	0.50007(14)	0.0281(6)
O6	1	0.3055(3)	0.5000	0.50497(19)	0.0289(9)
O7	1	0.5000	0.14949(17)	0.5000	0.0249(8)
Ca	0.982(3)	0.48964(12)	0.0000	0.29394(7)	0.0509(5)
Na	0.134(5)	0.2320(16)	0.4336(8)	0.2687(10)	0.090(7)[a]
Ow1	0.082(6)	0.431(2)	0.1112(15)	0.3071(15)	0.023(9)[a]
Ow2	0.865(7)	0.5244(5)	0.12614(19)	0.30172(18)	0.109(3)
Ow3	0.732(10)	0.4440(7)	0.0000	0.4246(3)	0.082(3)[a]
Ow30	0.171(9)	0.540(2)	0.0000	0.4219(12)	0.041(8)[a]
Ow4	0.165(14)	0.652(4)	0.5000	0.148(3)	0.20(3)[a]
Ow40	0.510(10)	0.6354(7)	0.0000	0.3739(6)	0.087(4)
Ow5	0.081(8)	0.441(3)	0.5000	0.338(2)	0.015(11)[a]
Ow50	0.930(10)	0.5724(6)	0.5000	0.3305(3)	0.145(4)
Ow6	0.780(11)	0.3667(6)	0.5000	0.3022(5)	0.129(4)
Ow7	0.610(7)	0.3335(5)	0.0778(3)	0.3036(3)	0.108(3)
Ow70	0.280(10)	0.6604(18)	0.0641(12)	0.3261(13)	0.197(13)[a]

[a] Positions were refined isotropically

Table 2 Atomic displacement parameters for stilbite

Atom	U_{11}	U_{22}	U_{33}	U_{12}	U_{13}	U_{23}
T11	0.0094(5)	0.0192(5)	0.0160(4)	0.0006(4)	–0.0002(4)	0.0000(4)
T12	0.0095(5)	0.0178(5)	0.0166(5)	–0.0002(4)	0.0012(4)	0.0010(4)
T2	0.0117(5)	0.0129(4)	0.0183(5)	–0.0014(4)	0.0000(4)	–0.0007(4)
T3	0.0081(4)	0.0158(4)	0.0168(4)	–0.0013(4)	0.0009(3)	–0.0004(4)
T4	0.0083(6)	0.0247(7)	0.0208(7)	0	0.0001(5)	0
O11	0.0219(14)	0.0299(13)	0.0306(13)	–0.0038(12)	–0.0114(11)	0.0032(11)
O12	0.0233(14)	0.0323(14)	0.0329(14)	0.0083(12)	0.0073(11)	0.0018(11)
O21	0.0252(14)	0.0327(14)	0.0318(14)	–0.0048(12)	–0.0055(11)	0.0161(11)
O22	0.0280(15)	0.0403(15)	0.0323(14)	0.0025(13)	0.0074(12)	0.0192(12)
O31	0.0331(16)	0.0319(14)	0.0312(14)	–0.0015(13)	0.0062(12)	–0.0092(12)
O32	0.0324(15)	0.0277(14)	0.0280(13)	–0.0015(12)	–0.0060(12)	–0.0058(11)
O4	0.0136(12)	0.0379(14)	0.0294(13)	–0.0021(12)	0.0041(10)	0.0000(11)
O5	0.0149(13)	0.0243(12)	0.0450(14)	–0.0074(11)	–0.0037(11)	0.0025(12)
O6	0.027(2)	0.0163(16)	0.043(2)	0	–0.0012(17)	0
O7	0.0129(17)	0.0259(18)	0.0362(19)	0	0.0022(15)	0
Ca	0.0886(13)	0.0267(7)	0.0368(8)	0	–0.0211(7)	0
Ow2	0.239(7)	0.044(2)	0.042(2)	–0.060(3)	–0.010(3)	0.0068(18)
Ow3	0.172(10)	0.038(4)	0.036(4)	0	0.003(4)	0
Ow40	0.056(7)	0.090(8)	0.114(9)	0	–0.066(6)	0
Ow50	0.319(11)	0.040(3)	0.073(4)	0	–0.110(5)	0
Ow6	0.103(8)	0.127(7)	0.159(8)	0	0.063(6)	0
Ow7	0.110(6)	0.102(5)	0.113(5)	0.064(4)	0.046(4)	0.034(4)

Thermogravimetry

Thermogravimetric measurements were carried out using TG-50 of Mettler TA3000 System. Two types of the measurements, scanning heating and isothermal, were carried out. First, the powder sample of 70.8 mg was measured at a heating rate of 2 °C min^{-1} from 20 to 610 °C. These data were used for the evaluation of the water content in the stilbite formula. Second, the fine powder of sample was heated at 10 °C min^{-1} from room temperature to the specified temperature and then kept until the sample mass becomes constant. Furnice with the sample inside is not isolated from the air around. The humidity inside the furnace is equalized with the air in the room during the long isothermal measurements, and the mass loss at different temperatures fits the equilibrium function $m(T)_{P=\text{const}}$. The experiment is rather long, and we change the sample each day in order to diminish the value of a drift, starting every new experiment again from room temperature. These measurements were carried out at 35, 50, 65, 80 °C (sample mass 25.852 mg); 95, 110, 125, 140, 155 °C (25.885 mg); 170 and 290 °C (25.950 mg); 200, 215, 230 °C (27.108 mg); 230, 245, 260 °C (27.191 mg); 320, 350, 380, 395, 410, 440 °C (26.258 mg). Temperature interval from 110 to 125 °C have shown very large change in the mass loss, and we repeated isothermal measurements with the temperature step of 1 °C, sample mass was 26.601 mg.

X-ray powder diffraction

Variable-temperature X-ray powder diffraction data for stilbite were obtained using Stoe STADI MP diffractometer equipped with Eurotherm 2416 high-temperature device, $CuK\alpha_1$ radiation (40 kV, 40 mA). The powdered sample was loaded into a silica glass capillary of 0.3 mm diameter and was placed in a high-temperature equipment. The temperature was increased by 1 °C min^{-1} to the desired values, and a dwell time of 10 min was used before each measurement. A linear position-sensitive detector (PSD) was employed for powder diffraction data measurement.

The first series was with the points at 50, 75, and 100 °C, then to 250 °C with the step of 10 °C, and finally up to 400 °C with the step of 25 °C. The PSD was stepped in 0.25° intervals between 8° and 40° in 2θ with counting time of 40 s per step. The capillary was spun during the measurement to provide the better powder averaging. The refinement of UC parameters was performed using the GSAS package [15] and the EXPGUI graphical interface [16]. The pseudo-Voigt function was used to model

Table 3 T–O distances (Å) and T–O–T angles (°) in stilbite

Bond distances/Å	
T11–O31	1.618(2)
T11–O4	1.626(2)
T11–O21	1.629(2)
T11–O11	1.639(2)
Mean	1.628
T12–O22	1.647(2)
T12–O12	1.657(2)
T12–O32	1.660(2)
T12–O4	1.663(2)
Mean	1.657
T2–O6	1.6188(9)
T2–O32	1.634(2)
T2–O31	1.638(2)
T2–O5	1.654(2)
Mean	1.636
T3–O22	1.602(2)
T3–O5	1.618(2)
T3–O21	1.621(2)
T3–O7	1.6352(15)
Mean	1.619
Bond angles/°	
T4–O11–T11	140.57(15)
T4–O12–T12	144.45(16)
T3–O21–T11	147.95(16)
T3–O22–T12	156.17(17)
T11–O31–T2	147.63(16)
T2–O32–T12	141.84(15)
T11–O4–T12	141.87(15)
T3–O5–T2	143.33(15)
T2–O6–T2	176.1(3)
T3–O7–T3	135.6(2)
Mean	146.63[a]

* The mean value was calculated with weights (multiplicity of O-positions)

the peak profile. Bias of zero point for the counter and reflection shift were corrected for the silicon reference sample. Structure solution of our sample (see Tables 1, 2, 3, and 4) was used as the starting model for the structure refinement, with variations in the sites of Si and O atoms and with the limitations in the Si–O and O–O distances in the tetrahedra. The mass loss after thermogravimetry was used to correct the occupancy of H_2O sites.

The second series of the measurements with the temperature step of 1 °C was carried out in the temperature range of 150–180 °C, where the changes in the UC parameters were very large in the first series. At the very start of the second series at 150 °C, the sample was kept for

Table 4 Environment of extraframework positions in stilbite (distances < 3 Å)

Bond distances	
Ca–Ow1(2×)	2.19(3)
Ca–Ow2(2×)	2.349(3)
Ca–Ow3	2.413(6)
Ca–Ow30	2.37(2)
Ca–Ow4	2.19(6)
Ca–Ow40	2.426(8)
Ca–Ow5	2.54(4)
Ca–Ow50	2.361(5)
Ca–Ow6	2.611(7)
Ca–Ow7(2×)	2.559(6)
Ca–Ow70(2×)	2.65(2)
Na–O11	2.529(17)
Na–O11	2.643(16)
Na–Ow70	1.42(3)
Na–Ow6	2.19(2)
Na–Ow70	2.24(3)
Na–Ow6	2.27(2)
Na–OW40	2.60(2)
Na–OW70	2.77(2)
Na–Na	0.83(3)
Na–Na	2.42(3)
Na–Na	2.56(3)
Ow1–Ow2	1.30(3)
Ow1–Ow3	2.91(3)
Ow1–Ow4	2.45(4)
Ow1–Ow7	1.46(3)
Ow2–Ow7	2.740(9)
Ow2–Ow70	2.20(2)
Ow3–Ow30	1.30(3)
Ow3–Ow30	2.74(2)
Ow3–Ow4	1.82(6)
Ow3–Ow40	2.763(14)
Ow3–Ow7(2×)	2.970(9)
Ow4–Ow7(2×)	1.67(3)
Ow5–Ow50	1.80(4)
Ow5–Ow6	1.18(4)
Ow6–Ow70(2×)	2.59(2)
Ow7–Ow7	2.836(12)
Ow7–Ow7	2.947(14)
Ow30–Ow30	2.99(5)
Ow30–Ow4	2.87(6)
Ow30–Ow40	1.56(3)
Ow30–Ow70(2×)	2.65(3)
Ow40–Ow70(2×)	1.49(2)
Ow50–Ow6	2.834(12)
Ow70–Ow70	2.33(4)

30 min. The diffraction pattern was measured in the angle range of 18–24.5° 2θ.

Results and discussion

Mass loss

Mass loss at scanning heating is shown in Fig. 1. There are three peaks of dehydration: at 173 °C (high and narrow), 227 °C (broad), and 450 °C (small). It is the first peak that is attributed to the phase transition into stilbite B. The second peak is due to the conventional regular dehydration [17]. The third one is due to the thermal amorphization of stilbite. Heated to this temperature, the sample does not adsorb the water again after cooling down to room temperature, and its X-ray powder diffraction pattern contains weakened reflections, if any.

Mass of stilbite after isothermal measurements is shown in Fig. 2. Each point was kept for 1–2 h to reach the constant mass. No drastic changes in the time of equilibration were seen for different temperatures. It is quite different from the similar experiments for heulandite and natrolite. Heulandite transforms at dehydration into heulandite B (the first-order phase transition), and the time of equilibration at the transition point grows up to 9 h [18]. Natrolite also has phase transition at dehydration, undergoing into completely dehydrated phase, and the time of equilibration in our experiments was too large to wait the completion of the transition [17].

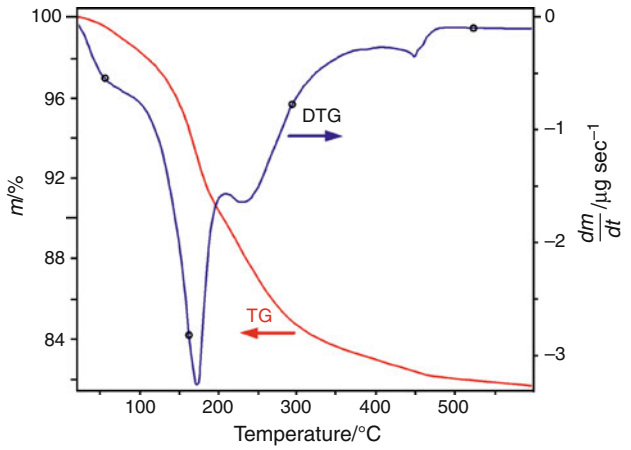

Fig. 1 Thermogravimetric results for stilbite at scanning heating

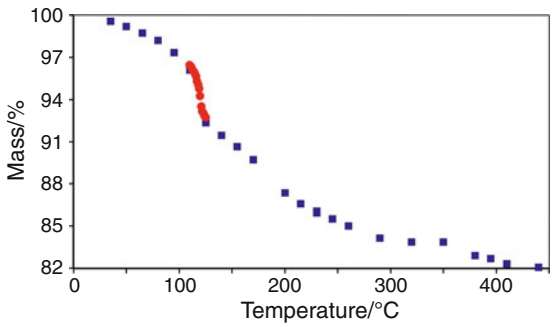

Fig. 2 Isothermal measurements of the mass loss for stilbite equilibrated with room humidity

The change in the mass is the greatest between 110 and 125 °C. It corresponds to the first (high and narrow) peak in Fig. 1, attributed to the phase transition at dehydration, but occurs at lower temperature (~115 °C) as compared with scanning heating (173 °C). This is a usual phenomenon for the dehydration at scanning heating and isothermal conditions [19]. The results of the second series with the step of 1 °C show clearly that there is no jump in the equilibrium mass loss. Line $m(T)$ is steep and continuous, rather than jump-like. At least, we can fit these points to a smooth curve. This result does not support the idea of the first-order phase transition in our stilbite.

Changes in the structure

The powder diffraction pattern for various temperatures is shown in Fig. 3. Reflections (−102), (102), (031), (013), (−142), and (142) are forbidden by the *F*-centered UC. They are indicated in the upper part of the Figure. First traces of reflections (−142) and (142) become detectable near 160 °C. The indexes of the reflections indicate that the original face-centered *F* lattice transforms into base-centered *A* one, but remains monoclinic up to the highest temperature in the experiment. Starting from 160 °C, the UC parameters were refined for the space group *A*2/*m*, with corresponding changes in the structure model. The UC parameters as functions of temperature are shown in Fig. 4. Most significant changes are there in the temperature range from 160 to 180 °C. The change in volume is of 2.24% between 160 and 170 °C and 3.5% between 160 and 180 °C. This value is very close to that found by Cruciani et al. [11], i.e., 3.24%, and they found the contraction caused by the phase transition accompanied with the increasing symmetry. The transition from stilbite A (*F*2/*m*) into stilbite B (*Amma*) was described. Contrary, in our sample we did not found the increase in symmetry, but from *F*2/*m* into presumably *A*2/*m*.

The second series of the measurements in the temperature range from 150 to 180 °C with the step of 1 °C in temperature did allow us to identify most accurately the point of symmetry change. The transition point was detected as the point where the (−142) and (142) reflections forbidden in the *F*-UC have appeared. Peak intensity and its position were defined using PROFIT software [20].

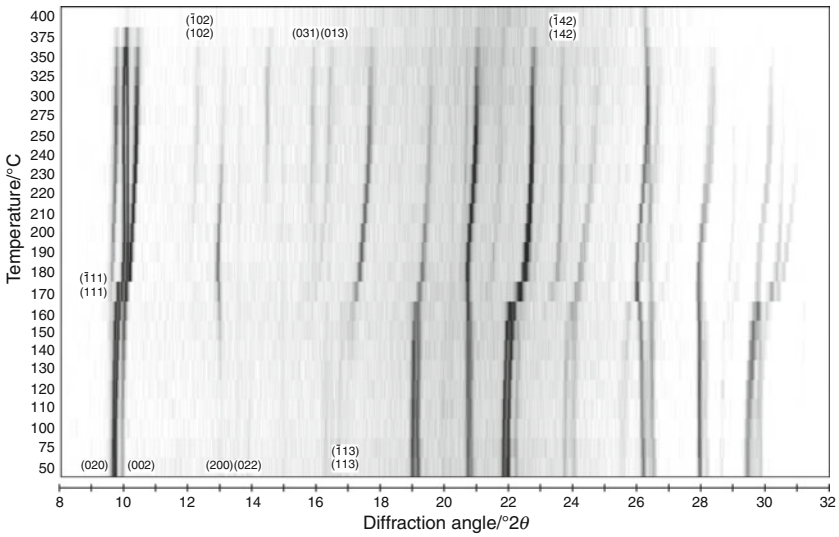

Fig. 3 X-ray powder diffraction pattern of stilbite at heating

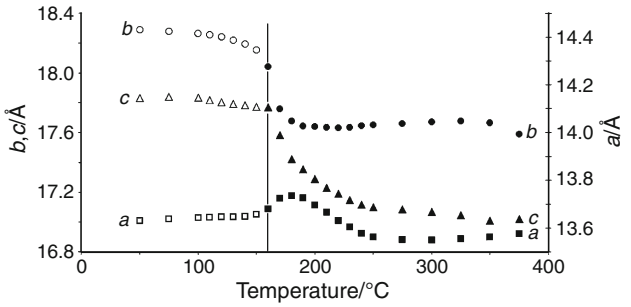

Fig. 4 Unit cell parameters of stilbite under heating over the whole temperature range. *Open marks* refinement starting from *F*2/*m*; *filled marks* refinement starting from *A*2/*m*

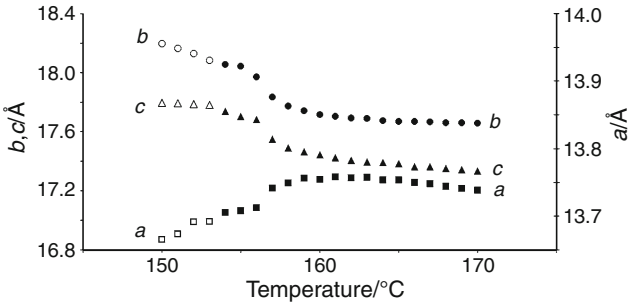

Fig. 5 Unit cell parameters of stilbite under heating in the vicinity of the phase transition. *Open marks* refinement starting from *F*2/*m*; *filled marks* refinement starting from *A*2/*m*

The reflections were detected for certain ($I > 3\sigma$) at 154 °C. The UC parameters in the range of 150–180 °C are shown in Fig. 5. Open marks indicate the parameters for space group *F*2/*m* and filled marks are for *A*2/*m*. The figure makes evident the gradual changes in the structure, contrary to the step-wise first-order phase transition described in [11].

Comparison with literature data

To clarify the reason of the contradiction between our results and those by [11], it is necessary to compare how the experiments differ from one another in the both works.

The samples are $Ca_{3.16}Na_{1.81}K_{0.22}Ba_{0.015}Sr_{0.14}Mg_{0.02}[Fe^{3+}_{0.005}Al_{8.665}Si_{27.32}O_{72}]\cdot 30H_2O$ in [11] and $Ca_{3.98}Na_{1.10}[Al_{9.07}Si_{26.93}O_{72}]\cdot 29.0H_2O$ in this work. The effects of the Al–Si ratio and their distribution among the tetrahedra were not described in literature. The increase in the number of sodium cations was reported to affect the symmetry of the mineral. Sites of cations in Ca-rich species are "partially occupied by water, so calcium can peacefully remain on the mirror plane, and symmetry is *F* 2/*m* 2/*m* 2/*m*" [10, p. 286]. Our sample is more rich in Ca than that in [11], and our sample should be of higher symmetry, but this is not the case. Thus, the difference in chemical composition cannot explain the difference in the thermal properties.

Both structure measurements were carried out at various temperatures in situ, with the sample inside 0.3 mm capillary axially spun during data collection. Experimental technique is synchrotron radiation powder diffraction with a wavelength of 1.488 Å in [11], and X-ray powder diffraction with a wavelength of 1.54059 Å in this work. Such a difference implies not to result in the order of the phase transition and symmetry changes.

Important is the difference in temperature program. Cruciani et al. [11] used the temperature step of 30 °C in the first series and 6 °C in the second one, with the total time between points of about 5 min. We used the steps of 10 and 25 °C in the first series and 1 °C in the second one, with the total time between points of about 85 min. Such a long duration in our experiments did allow the water content of the sample to be very close to the equilibrium. The time of equilibration in our TG experiments ranged mainly from 1 to 2 h. The diffraction patterns at 422 and

429 K in [11] were refined with a large R value. It was considered a manifestation of the first-order phase transition. We explain this large R value with significant changes in the UC parameters during the measurement, because 422 and 429 K fall into the range of the greatest change in sample mass. Indeed, the diffraction pattern cannot be fitted with low R value, if the sample changes significantly during the time of data collection. We did not find significant increasing in R value in our quasi-equilibrium sample.

Starting models for the structure refinement in [11] were borrowed in literature, different for $T < 416$ [21, 22] and $T > 422$ K [23]. We used the structure solution for our own sample for all temperatures. The latter is preferred because the change in the symmetry and UC parameters of starting model itself leads to the change in the symmetry and UC parameters of the refined structure.

Conclusions

We have investigated the thermal dehydration of stilbite and found out that (1) the changes in structure are gradual and (2) the structure remains monoclinic with the change in symmetry from *F2/m* to presumably *A2/m*.

In investigating the dehydration of zeolites, it is very important to plan the experiments in such a way that the water content of the sample changes very slowly during the sample preparation and must be nearly constant during the data collection. Dehydration and the contraction of the UC during the data collection corrupt the results. Fast dehydration can break the framework. Probably, similar case was reported for thermal dehydration of the samples of heulandite–clinoptilolite series [24].

Acknowledgements This work was supported by the Russian Foundation for Basic Research (grant # 10–05–00483).

References

1. Breck DW. Zeolites molecular sieves, structure, chemistry and use. New York: Wiley; 1974.
2. Meier WM, Olson DH. Atlas of zeolite structure types. Pittsburg: Polycrystal Book Service; 1978.
3. Rinaldi R. Zeolites. In: Frye K, editor. The encyclopedia of mineralogy. Stroudsburg: Hutchinson Ross Pub Co; 1981. p. 522–32.
4. Van Reeuwijk LP. The thermal dehydration of natural zeolites. Wageningen: Mededelingen Landbouwhogeschool; 1974.
5. Milligan WO, Weiser HB. Mechanism of the dehydration of zeolites. J Phys Chem. 1937;41:1029–40.
6. Smykatz-Kloss W. Application of differential thermal analysis in mineralogy. J Therm Anal Calorim. 1982;23:15–44.
7. Joshi MS, Rao PM, Choudhari AL, Kanitkar RG. Thermal behaviour of natural stilbite crystals. Thermochim Acta. 1982;58:79–86.
8. Yörükoğulları E, Yılmaz G, Dikmen S. Thermal treatment of zeolitic tuff. J Therm Anal Calorim. 2010;100:925–8.
9. Snellings R, Mertens G, Elsen J. Calorimetric evolution of the early pozzolanic reaction of natural zeolites. J Therm Anal Calorim. 2010;101:97–105.
10. Gottardi G, Galli E. Natural zeolites. Berlin: Springer-Verlag; 1985.
11. Cruciani G, Artioli G, Gualtieri A, Stahl K, Hanson JC. Dehydration dynamics of stilbite using synchrotron X-ray diffraction. Am Miner. 1997;82:729–39.
12. Sheldrick GM. A short history of SHELX. Acta Cryst. 2008;A64:112–22.
13. Mortier WJ, Pluth JJ, Smith JV. Positions of cations and molecules in zeolites with the mordenite-type framework. II. Dehydrated hydrogen-ptilolite. Mater Res Bull. 1975;10:1317–26.
14. Hajdo F. Revised parameters of the analytic fits for coherent and incoherent scattered X-ray intensities of the first 36 atoms. Acta Cryst. 1972;A28:250–2.
15. Larson AC, Von Dreele RB. General Structure analysis system (GSAS). Los Alamos National Laboratory Report LAUR 86–748; 2000.
16. Toby BH. EXPGUI, a graphical user interface for GSAS. J Appl Cryst. 2001;34:210–3.
17. Drebushchak VA. Isobaric zeolite dehydration. Geochem Int. 1990;27(8):115–20.
18. Drebushchak VA. Thermogravimetric investigation of the phase transition in the zeolite heulandite at dehydration. Thermochim Acta. 1990;159:377–81.
19. Dementiev SN, Drebushchak VA. Dehydration of zeolites at scanning heating. Geochem Int. 1992;29(9):1361–7.
20. Zhurov VV, Ivanov SA. PROFIT computer program for processing powder diffraction data on an IBM PC with a graphic user interface. Crystallogr Rep. 1997;42(2):202–6.
21. Galli E. Refinement of the crystal structure of stilbite. Acta Cryst. 1971;B27:833–41.
22. Quartieri S, Vezzalini G. Crystal chemistry of stilbites: structure refinement of one normal and four chemically anomalous samples. Zeolites. 1987;7:163–70.
23. Alberti A, Rinaldi R, Vezzalini G. Dynamics of dehydration in stilbite-type structures; stellerite phase B. Phys Chem Miner. 1978;68:880–99.
24. Armbruster T, Gunter ME. Stepwise dehydration of heulandite-clinoptilolite from Succor Creek, Oregon, U.S.A.: a single-crystal X-ray study at 100 K. Am Miner. 1991;76:1872–83.